Compendium of Current Total Ionizing Dose and Displacement Damage Results from NASA Goddard Space Flight Center and NASA Electronic Parts and Packaging Program

Alyson D. Topper, Michael J. Campola, Dakai Chen, Megan C. Casey, Ka-Yen Yau, Donna J. Cochran, Kenneth A. LaBel, Raymond L. Ladbury, Timothy K. Mondy, Martha V. O'Bryan, Jonathan A. Pellish, Edward P. Wilcox, Edward J. Wyrwas, and Michael A. Xapsos

***Abstract*-- Total ionizing dose and displacement damage testing was performed to characterize and determine the suitability of candidate electronics for NASA space utilization. Devices tested include optoelectronics, digital, analog, linear bipolar devices, and hybrid devices.**

Index Terms- Displacement Damage, Optoelectronics, Proton Damage, Single Event Effects, and Total Ionizing Dose.

I. INTRODUCTION

Long term radiation induced failure modes play a significant role in determining space system reliability. Therefore, the effects of total ionizing dose (TID) and displacement damage dose (DDD) need to be evaluated through ground-based testing in order to determine risk to spaceflight applications.

The test results presented here were gathered to establish the sensitivity of candidate spacecraft electronics to TID and/or DDD. Proton-induced degradation, dominant for most NASA missions, is a mix of ionizing (TID) and non-ionizing damage. The non-ionizing damage is commonly referred to as DDD. For similar results on single event effects (SEE), a companion paper has also been submitted to the 2017 IEEE NSREC Radiation Effects Data Workshop entitled: "Compendium of Current Single Event Effects Results from NASA Goddard Space Flight Center and NASA Electronic Parts and Packaging Program" by M. O'Bryan, et al. [1]

II. TEST TECHNIQUES AND SETUP

A. Test Method

Unless otherwise noted, all tests were performed at room temperature and with nominal power supply voltages. Based on the application, samples were tested in a biased or unbiased configuration. Functionality and parametric changes were measured either continually during irradiation (in-situ) or after step irradiations (for example: every 10 krad(Si), or every $1x10^{10}$ protons/cm^2).

B. Test Facilities – TID

TID testing was performed using MIL-STD-883, Test Method 1019.9 [2] unless otherwise noted as research. Dose rates used for testing were between 0.05 and 50 rad(Si)/s.

C. Test Facilities – Proton

Proton damage tests were performed on biased and unbiased devices. Table I lists the proton damage test facilities and energies used on the devices.

TABLE I: PROTON TEST FACILITIES

Facility	Proton Energy, (MeV)
University of California at Davis (UCD) Crocker Nuclear Laboratory (CNL)	63
Texas A&M University Cyclotron (TAMU)	45

III. TEST RESULTS OVERVIEW

Abbreviations for principal investigators (PIs) are listed in Table II. Abbreviations and conventions are listed in Table III. Summary of TID and DDD test results are listed in Table IV and VI. Summary of on-going TID test results are listed in Table V. Please note that these test results can depend on operational conditions.

TABLE II: LIST OF PRINCIPAL INVESTIGATORS

Abbreviation	Principal Investigator (PI)
DC	Dakai Chen
KY	Ka-Yen Yau
MCC	Megan C. Casey
MJC	Michael J. Campola

Manuscript received July 12, 2017. This work was supported in part by the NASA Electronic Part and Packaging Program (NEPP) and NASA Flight Projects.

Alyson D. Topper, Donna J. Cochran, Martha V. O'Bryan, and Edward P. Wilcox are with ASRC Federal Space and Defense, Inc. (AS&D, Inc.), work performed for NASA Goddard Space Flight Center, Code 561.4, Greenbelt, MD 20771 (USA), phone: 301-286-5489, email: Alyson.d.topper@nasa.gov.

Michael J. Campola, Megan C. Casey, Kenneth A. LaBel, Raymond L. Ladbury, Jonathan A. Pellish, Michael A. Xapsos are with NASA/GSFC, Code 561.4, Greenbelt, MD 20771 (USA), phone: 301-286-5427, email: Michael.j.Campola@nasa.gov.

Dakai Chen was with NASA Goddard Space Flight Center, Code 561, Greenbelt, MD 20771. He is now with Analog Devices Inc., Milpitas, CA 95035 (Tel: 408-432-1900 ext. 2191; Dakai.chen@analog.com).

Ka-Yen Yau was with ASRC Federal Space and Defense, Inc. (AS&D, Inc.)

Timothy K. Mondy is with NASA/GSFC, Code 562, Greenbelt, MD 20771 (USA), phone: 301-286-4253, email: timothy.mondy@nasa.gov

Edward Wyrwas is with Lentech, Inc., P.O Box 67155, Albuquerque, NM 87193, work performed for NASA Goddard Space Flight Center, Code 561.4, Greenbelt, MD 20771 (USA), phone: 301-286-5213, email: Edward.j.wyrwas@nasa.gov.

U.S. Government work not protected by U.S. copyright

Authorized licensed use limited to: Northeastern University. Downloaded on April 06,2022 at 20:27:09 UTC from IEEE Xplore. Restrictions apply.

TABLE III: ACRONYMS

A = Amp	LBNL = Lawrence Berkeley National Laboratory
BiCMOS = Bipolar – Complementary Metal Oxide Semiconductor	LDC = Lot Date Code
BJT = Bipolar Junction Transistor	LDO = Low Dropout
CMOS = Complementary Metal Oxide Semiconductor	LED = Light Emitting Diode
COTS = Commercial off-the-shelf	LDR = Low Dose Rate
CTR = Current Transfer Ratio	LDR EF = Low Dose Rate Enhancement Factor
DDD = Displacement Damage Dose	MeV = Mega Electron Volt
DDR = Double-Data-Rate (a type of SDRAM—Synchronous Dynamic Random Access Memory)	mA = milliamp
	MOSFET = Metal Oxide Semiconductor Field Effect Transistor
DTRA = Defense Threat Reduction Agency	Mrad = mega rad
DUT = Device Under Test	n/a = Not Available
ELDRS = Enhanced Low Dose Rate Sensitivity	Op-Amp = Operational Amplifier
FET = Field Effect Transistor	PI = Principal Investigator
GSFC = Goddard Space Flight Center	PMU = Pulse Measurement Unit
HDR = High Dose Rate	REAG = Radiation Effects & Analysis Group
h_{FE} = Forward Current Gain	RF = Radio Frequency
I_b = Base Current	SEE = Single Event Effects
I_c = Collector Current	SMD = Standard Microcircuit Drawings
I_{CE} = Collector-Emitter Current	Spec = Specification(s)
I_{os} = Offset Current	TAMU = Texas A&M University Cyclotron TAMU)
I_{off} = Dark Current	TID = Total Ionizing Dose
I_{OUT} = Output Current	UCD-CNL = University of California at Davis – Crocker Nuclear Laboratory
JFET = Junction Field Effect Transistor	

Authorized licensed use limited to: Northeastern University. Downloaded on April 06,2022 at 20:27:09 UTC from IEEE Xplore. Restrictions apply.

TABLE IV: SUMMARY OF TID TEST RESULTS

Part Number	Manufacturer	LDC	Device Function	Technology	PI	Results	App. Spec (Y/N)	Dose rate (mrad(Si)/s)	Degradation Level (krad (Si))
OPERATIONAL AMPLIFIERS									
AD654	Analog Devices	0630; (16-036)	Operational Amplifier	Bipolar	MJC	All parameters within specification up to 40 krad(Si)	Y	10	>40
PA02	APEX	1417; (16-033)	Operational Amplifier	Bipolar	DC	All parameters within specification up to 30 krad(Si)	Y	10	>30
LTC6268-10	Linear Technology	1433; (16-040)	Operational Amplifier	BiCMOS	DC	Minimal degradation up to 20 krad(Si)	Y	10	>20
TRANSISTORS									
2N2907AUB	Microsemi	n/a; (16-022)	PNP Transistor	Bipolar	KY	Gain degradation and failures at 45 krad(Si)	Y	10	45
JANTXV2N2222AUB	Microsemi	1523: (16-021)	NPN Transistor	Bipolar	KY	Gain out of specification at 55 krad(Si)	Y	10	45 < X < 55
JANTXV2N5115	Solitron	1449A; (16-039)	JFET	Bipolar	MJC	Minimal degradation up to 30 krad(Si)	Y	10	>30
MEMORY									
MT29F128G08AJAAAWP-ITZ	Micron	201504; (16-017)	Flash	CMOS	MJC	Large number of block errors at 30 krad(Si), Three devices showed unrecoverable chip select errors at 40 krad(Si)	N	0.7 – 10 rad(Si)/s	30
MT29F128G08AJAAAWP-ITZ	Micron	201504BYGGFZR.21; (16-018)	Flash	CMOS	MJC	Two devices showed unrecoverable chip select errors	N	0.7 – 10 rad(Si)/s	40
MB85AS4MT	Fujitsu	1638; (16-041)	Memory – Nonvolatile	CMOS & ReRAM	DC	No memory corruption observed. Peripheral circuitry failure observed > 20 krad(Si).	N	50 rad(Si)/s	20 < X < 50
MISCELLANEOUS									
AD2S80	Analog Devices	1452; (15-088)	Resolver to Digital Converter	BiCMOS	DC	Biased parts show functional failure between 18 and 30 krad(Si) at high dose rate and 12 to 18 krad(Si) at low dose rate.	Y	50 rad(Si)/s and 10	12<FF<18
UC1823A	Texas Instruments	1345; (15-062)	Pulse Width Modulator	BiCMOS	DC	All parameters within specification up to 30 krad(Si)	Y	10	> 30

Authorized licensed use limited to: Northeastern University. Downloaded on April 06,2022 at 20:27:09 UTC from IEEE Xplore. Restrictions apply.

Part Number	Manufacturer	LDC	Device Function	Technology	PI	Results	App. Spec (Y/N)	Dose rate (mrad(Si)/s)	Degradation Level (krad (Si))
SW15-802	Southwest Research Institute	1203, 1233; (16-007)	Optocoupler	Hybrid	MCC	One unbiased part showed an increase in dark current at 75 krad(Si). Parameters increased with dose for biased parts.	Y	5 – 50 rad(Si)/s	8 < X < 75
AD9364	Analog Devices	1401; (15-071)	Transceiver	CMOS	DC	Parameters within specification. Transmission power gain showed minimal degradation as dose increased	Y	100 rad(Si)/s	> 50

TABLE VI: SUMMARY OF ELDRS TEST RESULTS

Part Number	Manufacturer	LDC	Device Function	Technology /Package	PI	Results	App. Spec (Y/N)	Dose rate (mrad(Si)/s)	Degradation Level (krad (Si))
OPERATIONAL AMPLIFIERS									
RH1013MH	Linear Technology	0329A; (A214)	Operational Amplifier	Bipolar / TO-5 Metal Can	DC	Small levels of dose rate sensitivity in the I_B degradation. Parameters within spec.	Y	1	>20
								0.5	$40 < I_B \leq 60$
RH1013MJ8	Linear Technology	0305A; (A214)	Operational Amplifier	Bipolar /Ceramic DIP	DC	Small levels of dose rate sensitivity in the I_B degradation. Parameters within spec.	Y	1	>20
								0.5	$40 < I_B \leq 60$
RH1078MH	Linear Technology	0741A; (A224)	Operational Amplifier	Bipolar /TO-5	DC	Parameters remain within post-irradiation specification. Completed 11/22/2016.	Y	1	>40
								0.5	>30
RH1078W	Linear Technology	0325A; (A224)	Operational Amplifier	Bipolar /Flatpack	DC	Parameters remain within post-irradiation specification. Completed 11/22/2016.	Y	1	>40
								0.5	>30
RHF43B	STMicroelectronics	30820A; (A589)	Operational Amplifier	Bipolar / Ceramic Flat-8	DC	Minimal dose rate sensitivity. Parameters within spec. Completed 12/16/16	N	10	>100
								1	>50
								0.5	>50

Authorized licensed use limited to: Northeastern University. Downloaded on April 06,2022 at 20:27:09 UTC from IEEE Xplore. Restrictions apply.

Part Number	Manufacturer	LDC	Device Function	Technology /Package	PI	Results	App. Spec (Y/N)	Dose rate (mrad(Si)/s)	Degradation Level (krad (Si))
TRANSISTORS									
2N2222	Semicoa	1001; (13-024)	NPN Transistor	Bipolar / Engineering Samples	DC	Minimal degradation. All parameters within spec. [43]	N	10	>100
								1	>40
								0.5	>20
2N2222AJSR	Semicoa	1364; (13-017)	NPN Transistor	Bipolar	DC	LDR EF = 3.9 After 100 krad(Si). Completed in 2016.	N	10	$35 < h_{FE} < 45$
								5	$65 < h_{FE} < 90$
								1	>40
								0.5	>30
2N3811JS	Semicoa	1230; (13-063)	PNP Transistor	Bipolar	DC	No bias dependence.	N	1	$30 < h_{FE} < 50$
						Two devices exceeded specifications after 30 krad(Si). Completed 12/3/2016.		0.5	$60 < h_{FE} \leq 70$
2N2907	Semicoa	0932; (13-023)	PNP Transistor	Bipolar	DC	LDR EF = 1.78 after 100 krad(Si). Completed 12/3/2016.	N	10	$40 < h_{FE} < 50$
2N2369	Semicoa	J1934(wafer#); (13-020)	NPN Transistor	Bipolar	DC	All parameters within specification up to 100 krad(Si). Minimal LDR sensitivity. Completed Nov. 2016	N	1	> 100
2N3700JV	Semicoa	1109; (13-022)	NPN Transistor	Bipolar	DC	Strong bias dependence. Biased devices show enhanced degradation than grounded devices. Completed 6/23/2016.	N	1	$30 < h_{FE} < 40$
								0.5	>20
2N3700UBJV	Semicoa	J1935(wafer#); (13-021)	NPN Transistor	Bipolar	DC	Dose rate effect not evident at this stage. Completed 6/23/2016.	N	1	$10 < h_{FE} < 20$
								0.5	$15 < h_{FE} < 30$
2N5153	Semicoa	1013; (13-018)	PNP Transistor	Bipolar	DC	Minimal LDR EF. Completed 11/22/2016.	N	1	>50
2N5154	Semicoa	1023; (13-019)	NPN Transistor	Bipolar	DC	Minimal LDR EF. Completed 11/22/2016.	N	1	>50

Authorized licensed use limited to: Northeastern University. Downloaded on April 06,2022 at 20:27:09 UTC from IEEE Xplore. Restrictions apply.

Part Number	Manufacturer	LDC	Device Function	Technology /Package	PI	Results	App. Spec (Y/N)	Dose rate (mrad(Si)/s)	Degradation Level (krad (Si))
VOLTAGE REFERENCES/REGULATORS									
LM136AH2.5QMLV	National Semiconductor	200746K019; (A164)	Voltage Reference	Bipolar/3-LEAD TO-46	DC	Exhibits no LDR enhancement.	N	0.5	>70
LM317LTTR	Texas Instruments	0608; (A113)	Positive Voltage Regulator	Bipolar	DC	Parameters within specification. Observed LDR sensitivity for parts irradiated at 0.5 after 20 krad(Si).	N	0.5	> 70
LT1009IDR	Texas Instruments	0606; (A327)	Internal Reference	Bipolar	DC	Parameters within specification. Parts exhibit minimal LDR enhancement.	N	0.5	> 70
RHFL4913ESY332	STMicroelectronics	30828A; (A259)	Voltage Regulator	Bipolar/TO-257	DC	All parameters within specification. Minimal dose rate sensitivity. Completed 7/22/2016.	N	0.5	> 60
RHFL4913KP332	STMicroelectronics	30814B; (A258)	Voltage Regulator	Bipolar/Flat-16	DC	All parameters within specification. Minimal dose rate sensitivity. Completed 7/22/2016.	N	0.5	> 60
TL750M05CKTRR	Texas Instruments	0707; (A112)	LDO Positive Voltage Regulator	Bipolar/TO-263-3	DC	Minimal dose rate sensitivity.	N	0.5	> 70
MISCELLANEOUS									
LM139AWRQMLV	National Semiconductor	JM046X13; (A211)	Comparator	Bipolar	DC	Parameters within specification. Completed 11/22/2016.	Y	0.5	I_b > 75

Authorized licensed use limited to: Northeastern University. Downloaded on April 06,2022 at 20:27:09 UTC from IEEE Xplore. Restrictions apply.

TABLE V: SUMMARY OF DD TEST RESULTS

Part Number	Manufacturer	LDC	Device Function	Technology	PI	Results	App. Spec (Y/N)	Proton Fluence (/cm^2)
SW15-802	Southwest Research Institute	1203, 1233; (16-007)	Optocoupler	Hybrid	MCC	Increase of dark current and decrease of CTR with increasing fluence	Y	$6x10^{10}<I_{off}<3x10^{11}$
53111	Micropac	Q1614; (16-035)	Optocoupler	Hybrid	MJC	Some degradation in turn on time, leakage prevents turn off	Y	$3x10^{11}<I_{off}<4x10^{11}$
OPB848	Optek	n/a; (17-009)	Optocoupler	Hybrid	MJC	On-state collector current out of specification at $9.32x10^{10}< I_{Con} < 1.12x10^{11}$	Y	$9.32x10^{10}<I_{Con}<1.12x10^{11}$

Authorized licensed use limited to: Northeastern University. Downloaded on April 06,2022 at 20:27:09 UTC from IEEE Xplore. Restrictions apply.

IV. TEST RESULTS AND DISCUSSION

As in our past workshop compendia of GSFC test results, each device under test has a detailed test report available online at http://radhome.gsfc.nasa.gov [3] and at http://nepp.nasa.gov [4] describing in further detail the test method, conditions and monitored parameters, and test results. This section contains a summary of testing performed on a selection of featured parts.

A. AD9364, Analog Devices, RF Transceiver

The AD9364 is a commercial-off-the-shelf (COTS) high performance, highly integrated radio frequency (RF) Agile Transceiver designed for use in 3G and 4G base station applications. It is built on a commercial 65-nm CMOS process. TID testing was carried out on four samples at an average dose rate of 100 rad(Si)/s.

The device under test (DUT) was configured as a part of the AD-FMCOMMS4-EBZ evaluation platform. The AD-FMCOMMS4-EBZ evaluation platform interfaced with the ZedBoard. The ZedBoard contains the Zynq-7020 System-on-Chip (SoC), 512 MB DDR3, 256 Mb Quad-SPI flash, and 4 GB SD memory card. Figure 1 shows a photograph of the test setup on the bench, with the evaluation cards mated with the ZedBoard. Figure 2 shows the top and bottom view of the evaluation board. The AD9364 is circled. As shown, there are several other active components mounted on the bottom of the board. During irradiation, the entire ZedBoard was positioned behind lead brick shielding. We performed dosimetry at various locations behind the shielding, and determined that at a spot one inch away from the edge of the shielding, the total dose is negligible. However, approximately ½ inch away from the edge, the total dose will be a fifth of the total dose received by the DUT at the unshielded target. Therefore, the components on the evaluation card near the edge of the shielding accumulated approximately 5 - 10 krad(Si) during the exposure.

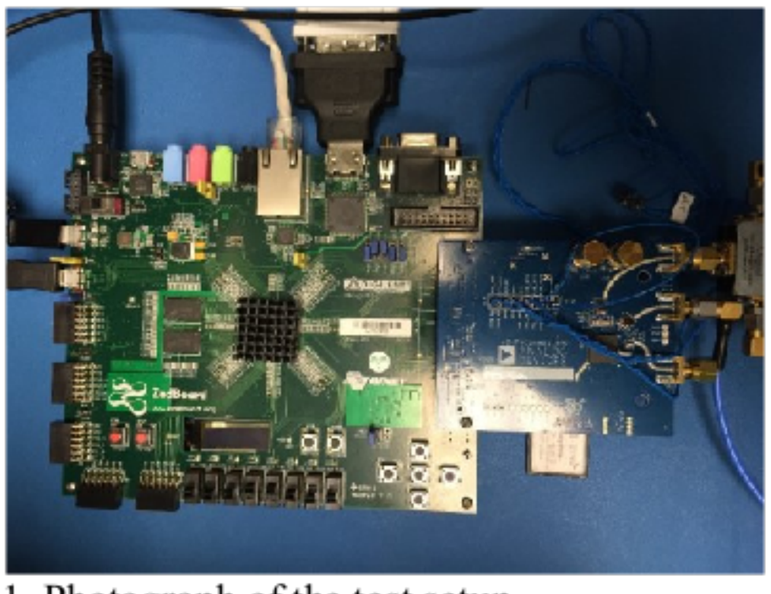

Fig. 1. Photograph of the test setup.

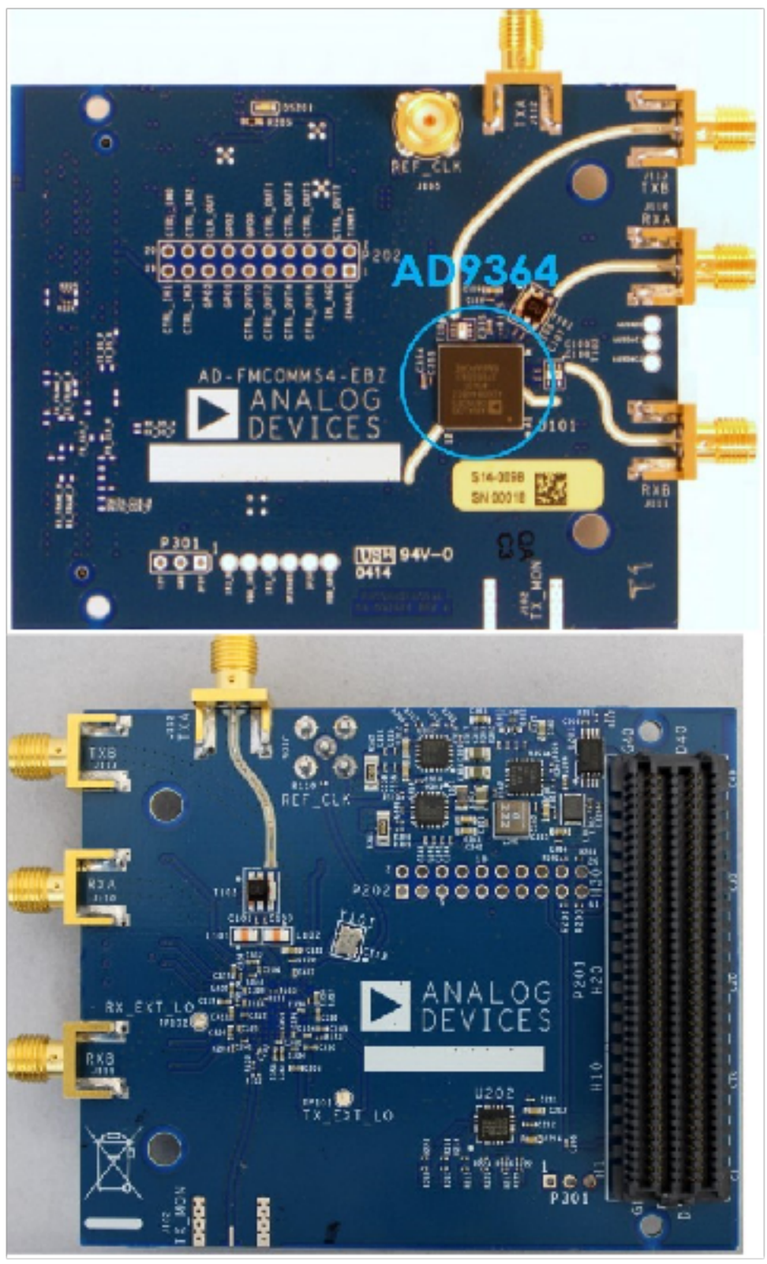

Fig. 2. Top and bottom view of the AD-FMCOMMS4-EBZ evaluation board.

The parts exhibited limited degradation in general. Most of the electrical parameters showed negligible change up to 50 krad(Si). The transmission power gain showed some degradation with increasing total dose. The gain degradation manifested visually through the image transmission tests. Figure 3 shows a pristine image and an image transmitted with a gain of 62 dB after 50 krad(Si). We show the results from two transmission operations. The second test, shown in Figure 3b, produced relatively fewer errors. In both cases, the transmitted image post-irradiation becomes pixelated due to the loss in power. Figure 3, third image, shows the pre-irradiation and post-irradiation image with a gain of 50 dB. The pixelation is reduced significantly. The pixelation issue disappears at a higher transmission power.

Authorized licensed use limited to: Northeastern University. Downloaded on April 06,2022 at 20:27:09 UTC from IEEE Xplore. Restrictions apply.

a. First b. Second c. Third

Fig. 3. Pre-irradiation (top) and post-irradiation (bottom) images transmitted after 50 krad(Si) for DUT2. The first and second images represent the first (a) and second (b) transmissions, respectively. The second transmission produced relatively fewer errors. The third image transmitted (c) with gain of 50 dB after 50 krad(Si) for DUT2.

B. 53111, Micropac, Optocoupler

The 53111 is a single-channel power MOSFET optocoupler rated for 90 V. It is available to Standard Microcircuit Drawings (SMD) specifications as 5962-9314001HPA. Displacement Damage testing was conducted on ten samples at CNL-UCD. To avoid part overstress a Keithley Pulse Measurement Unit (PMU) was used for pulse sweeping the device parameters, this also reduces internal heating of the device. During testing we saw two types of degradation on the optocoupler, increased turn on time delay and leakage on the output MOSFET.

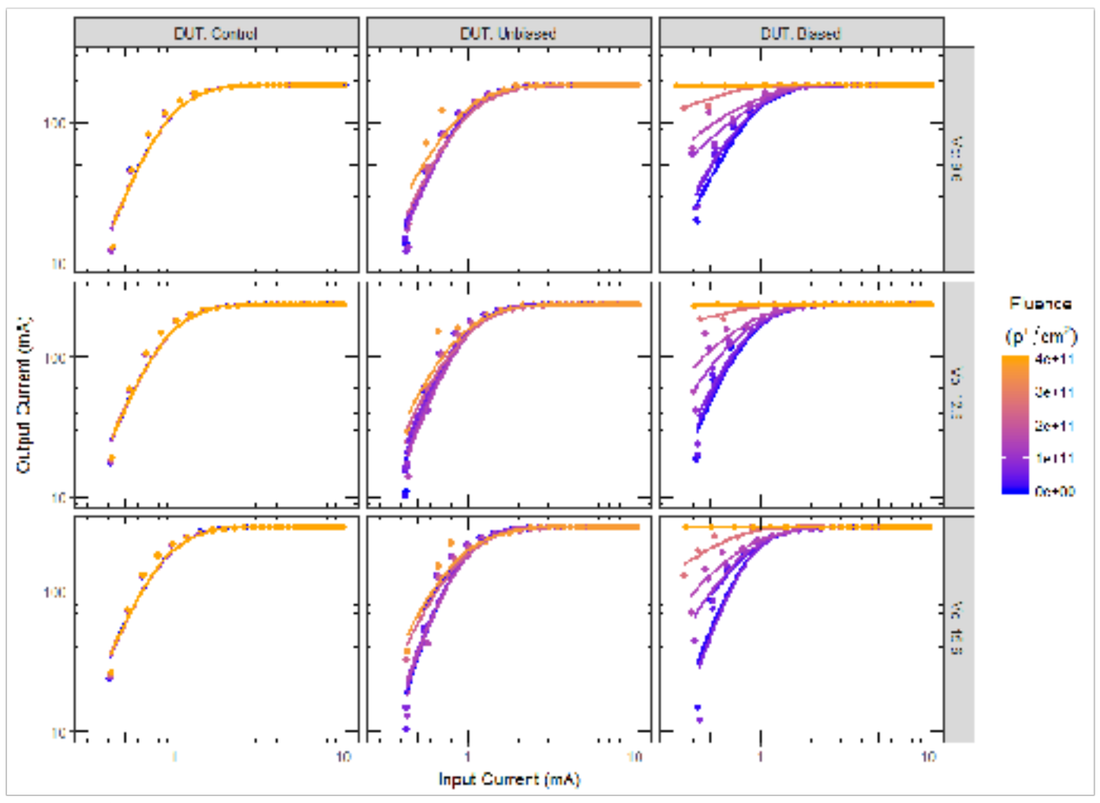

Fig. 4. Output current for a given input current using pulsed measurements.

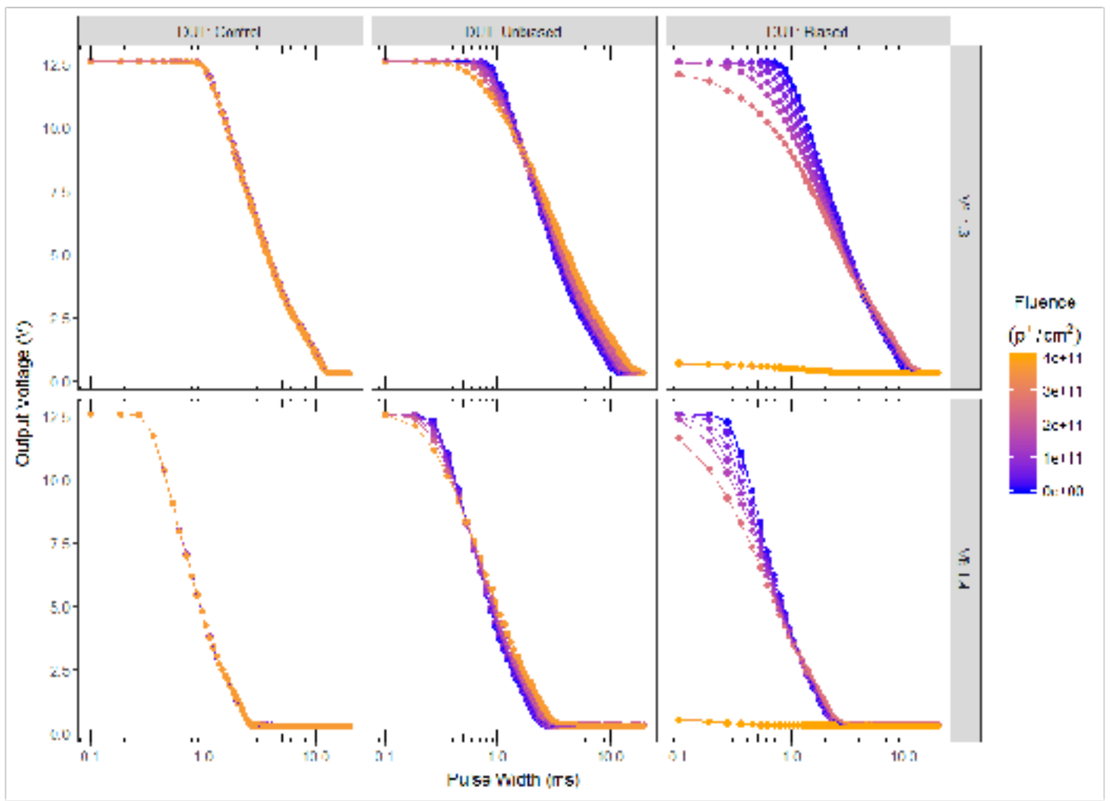

Fig. 5. Turn-on voltage for a given pulse width.

The degradation shown in Figure 4 details the biased parts as being more susceptible to proton exposure. At the final tested fluence step, the devices were permanently "on" independent of input current. This effect is attributed to the leakage path through the Metal Oxide Semiconductor Field Effect Transistor (MOSFET) stage of the device. This degradation remained present even as no bias was on the LED stage. Figure 5 however shows the delay in turn on time for given pulse widths synchronized on the drain of the MOSFET and high side of the LED. The delay is more pronounced for the unbiased devices, and therefore is suspected to be degradation of the LED and/or material that the light propagates through.

C. SW15-802, Southwest Research Institute, High Voltage Optocoupler

The SW15-802 is a ±6 kV optocoupler with hetero-junction LED structure. It employs low outgassing space-grade potting and coating. The internal high-voltage diode is glass-passivated and rated at 15 kV. Figure 6 shows a pin configuration for this uniquely packaged device. Southwest Research Institute designed this optocoupler as a replacement for a commercially-available radiation-tolerant optocoupler.

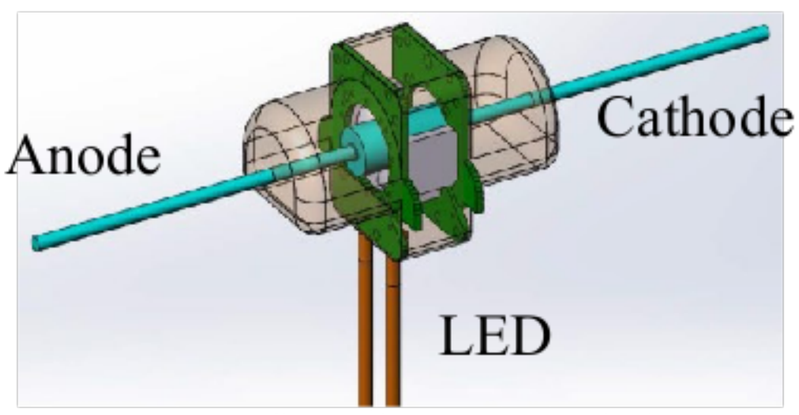

Fig. 6. Pin configuration and description.

TID testing was carried out on eight parts to a total dose of 150 krad(Si). The four unbiased parts, with all pins grounded, were irradiated first at a dose rate of 50 rad(Si)/s. Only small degradation was observed up to 75 krad(Si). After this dose step, the dark current parameter

Authorized licensed use limited to: Northeastern University. Downloaded on April 06,2022 at 20:27:09 UTC from IEEE Xplore. Restrictions apply.

for one part increased ten times from the pre-irradiation value. These results are shown in Figure 7. Only small increases in the CTR measurement were observed for LED current conditions of 10 mA and 20 mA. A large CTR increase was seen with an LED current of 0 mA, almost ten times the pre-radiation value.

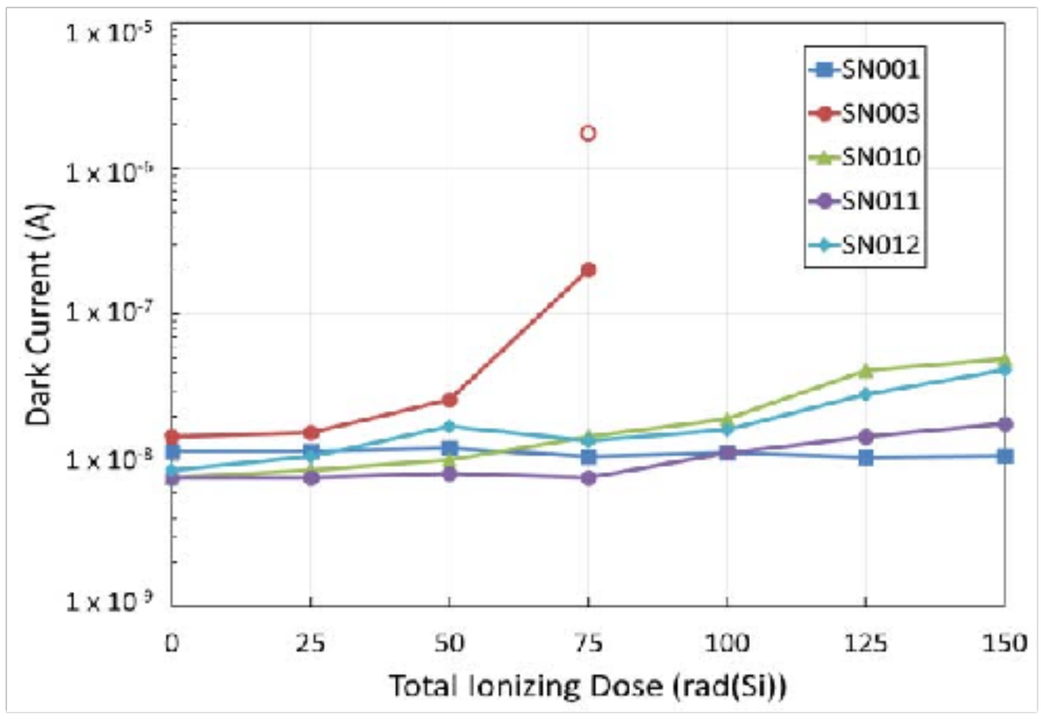

Fig. 7. Dark current versus TID for the parts irradiated unbiased.

The remaining four parts were biased at ±6.1 kV on the anode and cathode and no LED bias current. All four parts were irradiated together up to 7.6 krad(Si). At this point, the parts were drawing too much current for the 10 kV Stanford Research Systems power supply. One part was then irradiated at a time and the dose rate was reduced from 50 rad(Si)/s to about 5 rad(Si)/s. SN056 showed almost a thirty times increase in the dark current parameter at 7.6 krad(Si). The open circle shown for SN056 are measurements of the part that were taken four days later after a 60C annealing. There was some recovery, but the dark current still shows about a twenty times increase compared to the pre-rad value. This confirmed that the parts did experience some recovery from annealing, but most of the damage remained. The other three irradiated parts each had about 10x increase in dark current. Figure 8 shows the biased parts results for the dark current parameter. Similar results were seen in the biased parts for CTR as in the unbiased parts. At an LED current of 0 mA the CTR increased by thirty-eight times, while the LED current conditions of 10 mA and 20 mA only saw about a 5% increase.

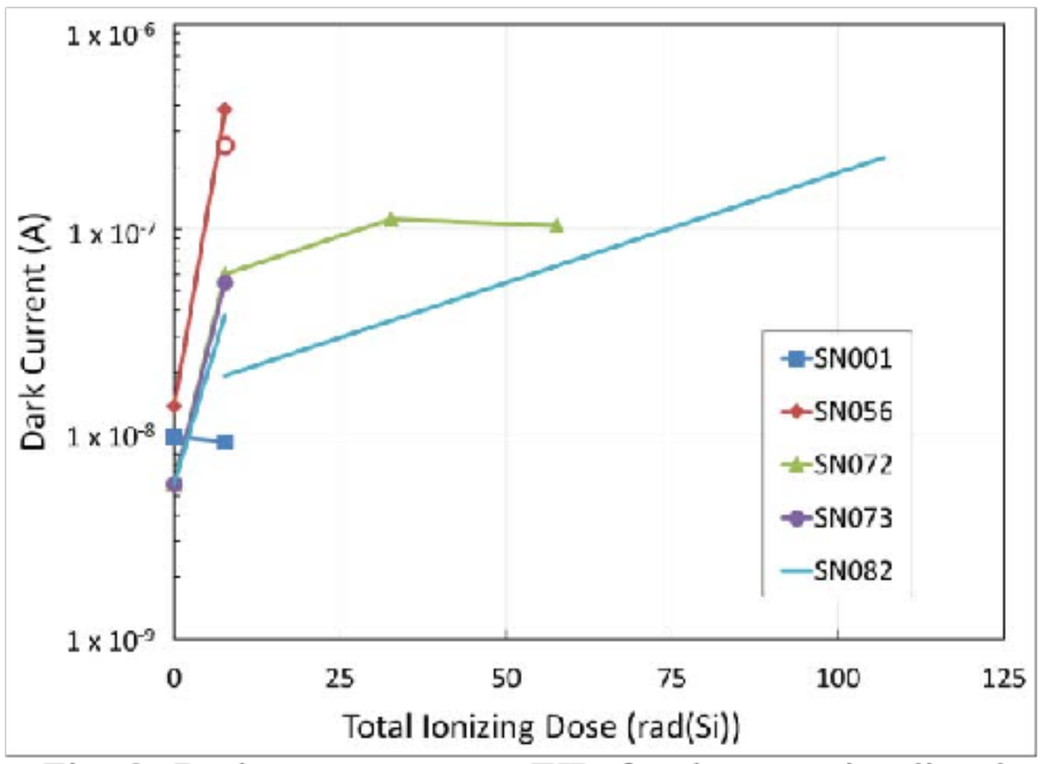

Fig. 8. Dark current versus TID for the parts irradiated while biased at ±6.1 kV.

Displacement damage testing was also conducted on eight parts at TAMU. Four parts were irradiated with diode and LED grounded and the remaining four parts were irradiated with the diode grounded but the LED biased at 20 mA. There were two control devices. The parts were irradiated in $6x10^{10}$ p/cm^2 steps up to a total fluence of $3x10^{11}$ p/cm^2.

In both the biased and unbiased parts, dark current increased as the proton fluence increased. Figures 9 and 10 show these test results. Similar results were also seen in the CTR parameter. CTR decreased as fluence increased when the LED current conditions were 10 mA and 20 mA but increased when the LED current was 0 mA. Only failure of this optocoupler was an unacceptable response as there was no defined specification limit.

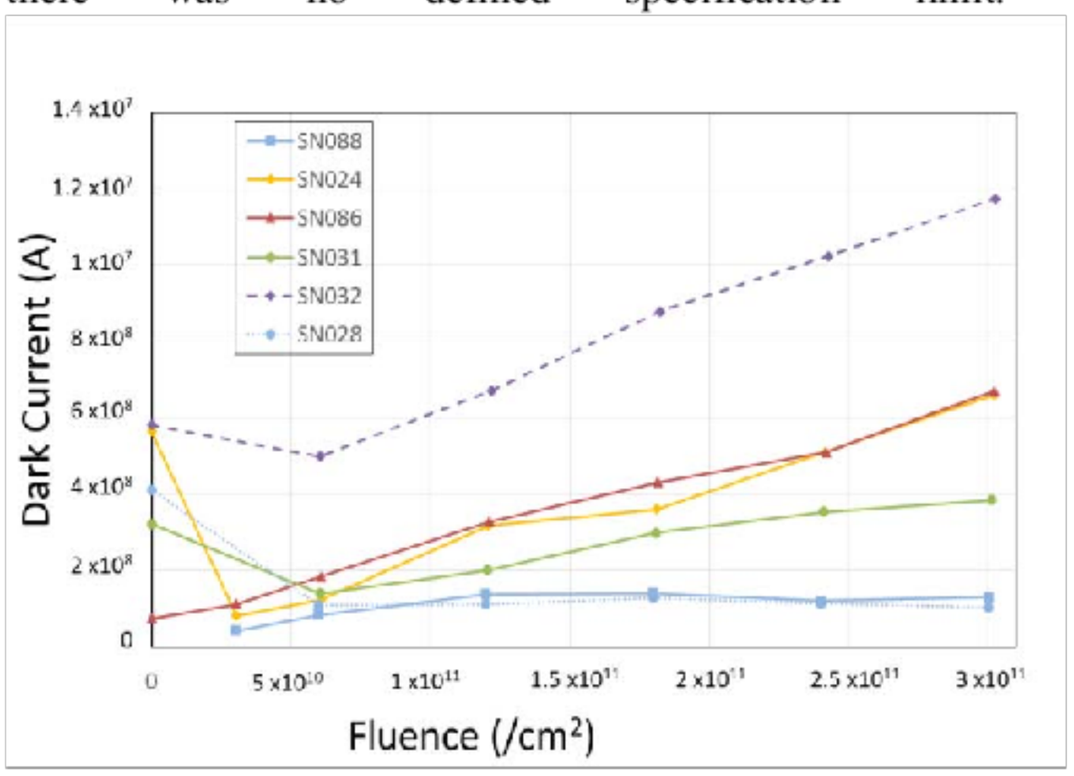

Fig. 9. Dark current as a function of proton fluence for the unbiased parts.

Authorized licensed use limited to: Northeastern University. Downloaded on April 06,2022 at 20:27:09 UTC from IEEE Xplore. Restrictions apply.

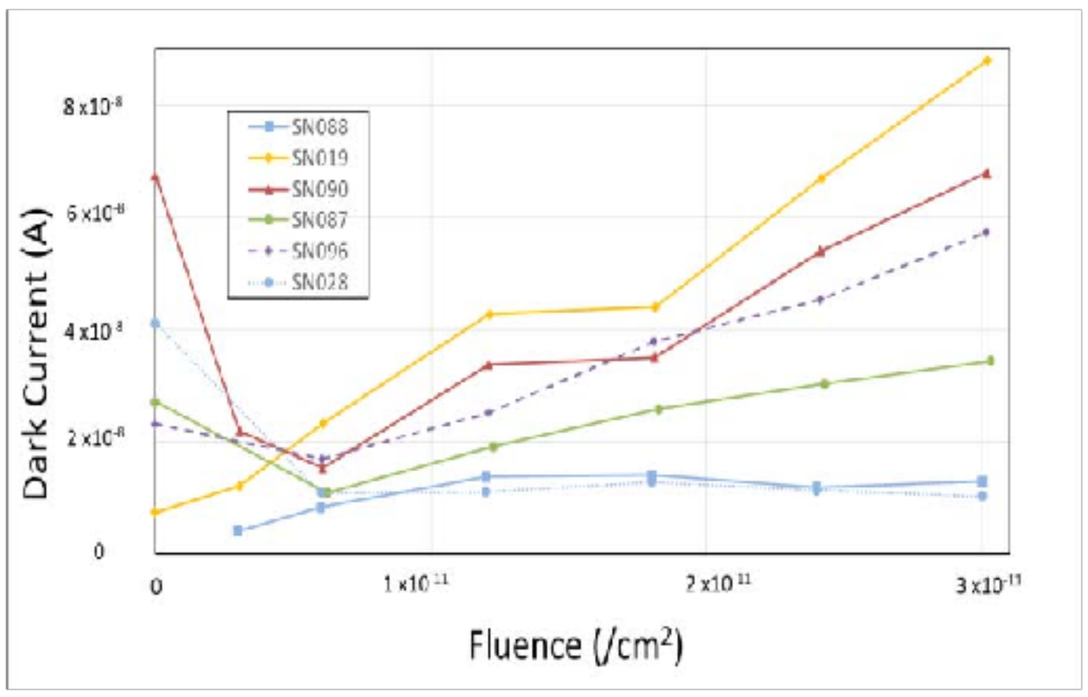

Fig. 10. Dark current as a function of proton fluence for the biased parts.

V. SUMMARY

We have presented data from recent TID tests on a variety of primarily commercial devices. It is the authors' recommendation that this data be used with caution due to many application/lot-specific issues. We also highly recommend that lot testing be performed on any suspect or commercial device. As in our past workshop compendia of GSFC test results, each DUT has a detailed test report available online describing in further detail, test method, TID conditions/parameters, test results, and graphs of data [3].

VI. ACKNOWLEDGMENT

The authors acknowledge the sponsors of this effort: NASA Electronic Parts and Packaging Program (NEPP), and NASA Flight Projects. The authors thank members of the Radiation Effects and Analysis Group (REAG) who contributed to the test results presented here: Melanie D. Berg, Stephen K. Brown, Martin A. Carts, Stephen R. Cox, James D. Forney, Yevgeniy Gerashchenko, Hak S. Kim, Anthony M. Phan, and Christina M. Seidleck.

The authors would also like to thank all external assistance in testing the high voltage optocoupler (SW15-802). We acknowledge Eric Young and Emanuel Hernandez of the Power group at NASA GSFC, code 563 and Carlos Urdiales, Armando De Los Santos, Dennis Guerrero, Steve Persyn, Mark Phillips, and Jessica Tumlinson, of Southwest Research Institute. Without their expertise and support, none of this work would have been possible.

VII. REFERENCES

[1] Martha V. O'Bryan, Kenneth A. LaBel, Carl M. Szabo, Dakai Chen, Michael J. Campola, Megan C. Casey, Jean-Marie Lauenstein, Edward J. Wyrwas, Steven M. Guertin, Jonathan A. Pellish, and Melanie D. Berg, "Compendium of Current Single Event Effects Results from NASA Goddard Space Flight Center and NASA Electronic Parts and Packaging Program," submitted for publication in IEEE Radiation Effects Data Workshop, Jul. 2017.

[2] Department of Defense "Test Method Standard Microcircuits," MIL-STD-883 Test Method 1019.9 Ionizing radiation (total dose) test procedure, June 7, 2013, https://landandmaritimeapps.dla.mil/Downloads/MilSpec/Docs/MIL-STD-883/std883.pdf.

[3] NASA/GSFC Radiation Effects and Analysis home page, http://radhome.gsfc.nasa.gov.

[4] NASA Electronic Parts and Packaging Program home page, http://nepp.nasa.gov.

Authorized licensed use limited to: Northeastern University. Downloaded on April 06,2022 at 20:27:09 UTC from IEEE Xplore. Restrictions apply.